

# Effect of Styrene-Butadiene-Styrene Block Copolymer on Fatigue Crack Propagation Behavior of Asphalt Concrete Mixtures

H. AGLAN, A. OTHMAN, L. FIGUEROA, AND R. ROLLINGS

The effect of styrene-butadiene-styrene (SBS) additive percentage on the fatigue crack propagation behavior of AC-5 asphalt concrete mixture was studied. Beams were prepared from AC-5 asphalt binder containing 6, 10, and 15 percent SBS by weight. Flexural fatigue tests were conducted on three identical specimens at each additive percentage. Parameters controlling the crack propagation process were evaluated—namely, the energy release rate and the change in work expended on damage formation and history-dependent viscous dissipation processes. The modified crack layer model was used to extract the specific energy of damage  $\gamma'$  characteristic of the mixture's resistance to crack propagation and the dissipative coefficient  $\beta'$ . It has been found that the 15 percent SBS mixture displayed superior fracture toughness as reflected in  $\gamma'$  and  $\beta'$ . As the additive percentage was increased, the fracture toughness of the mixture increased. Also, the ultimate strength and modulus increased. Within the range of additive percentage tested it appears that both the polystyrene endblocks and butadiene rubbery midblocks are working together to improve the ultimate strength and fracture toughness of the asphalt concrete mixture. Scanning electron microscope examination revealed an obvious change in the morphology of the fracture surface as the percentage of additive in the binder increased. This change is manifested in ridge formation in the binder-rich areas of the mixture. This change is also indicative of better adhesion between the binder and the aggregate as well as better cohesion within the binder, which in turn contributes to the increased toughness of the asphalt concrete mixture.

Polymer modifiers vary in function and effectiveness. Elastomers, which are at least to some extent derived from a diene chemical structure, will toughen asphalt and improve temperature viscoelastic properties. Plastomers, which come from nondiene chemicals, improve the high-temperature viscoelastic properties of softer asphalt, which has good intrinsic low-temperature properties (1, p. 39). The properties of asphalt mixtures can be improved by selecting modifiers in the proper molecular weight range and mixing the modifiers with asphalt mixtures appropriately. In addition, these modifiers must have solubility parameters close to those of the asphalt mixtures. One of the critical factors that should be considered for better rubber modified asphalt is the air void percentage in the total mix. The performance of the rubber modified asphalt mixture will be improved as this percentage is reduced (2,3). In general, the air void percentage depends on the load

capacity of the transportation facility being designed. Lower air void percentages can be obtained by increasing both the modifier and the asphalt binder content until the required value is reached (2).

Investigation into the effect of asphalt additives on pavement performance (4) has revealed that in general all additives improved their temperature susceptibility. Under stress control fatigue, using the phenomenological approach, which is based on the Wohler concept (5, p. 199), these workers concluded that styrene-butadiene-styrene (SBS) was one of the top additives among five tested [polyethylene, ethyl-vinyl acetate (Elvax), SBS (Kraton), styrene-butadiene rubber (latex), and carbon black] at  $-17.8^{\circ}\text{C}$  and  $20^{\circ}\text{C}$  ( $0^{\circ}\text{F}$  and  $68^{\circ}\text{F}$ ). However when the mixtures containing additives were aged at  $60^{\circ}\text{C}$  ( $140^{\circ}\text{F}$ ) for 7 days, their fatigue lifetime decreased considerably compared with their unaged counterparts. Under controlled displacement fatigue, using the Paris equation (6, p. 381;7), they also concluded that the SBS additive was considerably superior among those additives tested at  $0.56^{\circ}\text{C}$  ( $33^{\circ}\text{F}$ ). At  $25^{\circ}\text{C}$  ( $77^{\circ}\text{F}$ ) crack branching, which tends to redistribute the stress, causing main crack growth retardation, was observed.

In the current study, focus is placed on SBS (Kraton) because it has been found to be one of the most useful additives, particularly with low-penetration asphalt such as AC-5. Kraton consists of two different polymer blocks: hard polystyrene endblocks chemically crosslinked to soft rubbery midblocks in a three-dimensional rubber network. The hard polystyrene endblocks give Kraton rubber its high tensile strength and flow resistance at high temperature, whereas the rubbery midblocks are responsible for its elasticity, fatigue resistance, and flexibility at low temperatures. When Kraton rubber is mixed with hot asphalt, the polystyrene endblock domains begin to soften, allowing molecules into the asphalt while the rubbery midblocks start absorbing the asphalt's maltene fraction and swell to many times their initial volume. This swelling causes the SBS rubber phase to dominate the asphalt phase, resulting in a new modified asphalt binder possessing the principal characteristics of rubber. After the asphalt mixture is cooled, the polystyrene endblock domains reharden and form physical crosslinks with the rubbery midblocks, forming a strong, elastic, three-dimensional network again (8,9). It should be expected that this bonding action of the asphalt with the SBS rubber is largely influenced by the additive content percentage. Because this bonding action enhances the asphalt aggregate adhesion, it is of interest to study the effect of the additive percentage on both the macro- and micromechanical behavior

H. Aglan, Mechanical Engineering Department, Tuskegee University, Tuskegee, Ala. 36088. A. Othman and L. Figueroa, Civil Engineering Department, Case Western Reserve University, Cleveland, Ohio 44106. R. Rollings, USAE Waterways Experiment Station, 3909 Halls Ferry Road, Vicksburg, Miss. 39180.

of the asphalt concrete mixture. This effect is addressed in the current study.

The development of fatigue crack resistant pavements necessitates the thorough understanding of the combo-viscoplastic behavior of the binders (asphalt) and the additives (modifiers), which have been shown to be the major constituents influencing pavements' crack resistance. Recently, a methodology, the modified crack layer (MCL) model, has been developed (10, p. 53) to characterize the resistance of materials to fatigue crack propagation (FCP). The capability of this approach to discriminate the subtle effects introduced by different chemical structures and processing conditions has been demonstrated (10–13). The MCL model essentially addresses the difficulties encountered in the general applicability of the crack layer model (14,15). These difficulties are the identification and quantification of damage species associated with fatigue crack propagation in materials.

For stress control fatigue, the MCL model is expressed as

$$\frac{da}{dN} = \frac{\beta' \dot{W}_i}{\gamma' a - J^*} \quad (1)$$

where

$da/dN$  = cyclic crack speed,

$\dot{W}_i$  = change in work,

$J^*$  = energy release rate,

$a$  = crack length,

$\gamma'$  = candidate material parameter characteristic of the mixture's resistance to FCP, and

$\beta'$  = energy dissipative character of pavement.

In this paper, the parameters  $\gamma'$  and  $\beta'$  extracted from fatigue crack propagation experiments using the MCL model will be used to establish the effect of the SBS additive percentage on the fracture resistance of AC-5 asphalt concrete mixtures. In addition, the effect of additive percentage on the micromechanical behavior of the AC-5 asphalt concrete mixture is explored using scanning electron microscopy (SEM).

## EXPERIMENTAL METHOD

### Materials

AC-5 asphalt cement was used in this study with the following physical properties: penetration at 25°C (77°F) was 204 using (ASTM D-5), viscosity at 135°C (275°F) was 201 cSt using (ASTM 2170), viscosity at 60°C (140°F) was 461 poise using (ASTM 2171), and flash (Clev. Open Cup) using (ASTM 92) was 313°C (595°F). Crushed limestone aggregate and quartzitic sand were selected for the preparation of test specimens. The following Ohio Department of Transportation (ODOT Item 403) gradation was used (16):

Sieve Size	Total Passing (%)
½ in.	100
¾ in.	95
No. 4	59
No. 16	28
No. 50	9
No. 200	0

Kraton D4463 (SBS), which belongs to the general group of thermoplastic elastomers, was chosen as the modifier. It is

supplied in pellet form and requires mixing at temperatures between 160°C and 193°C (320°F and 380°F).

### Sample Fabrication

#### Preparation of Kraton-Asphalt Blends

The following blending sequence was used for the modified asphalt mixtures:

1. Asphalt cement was heated alone to 149°C (300°F).
2. The required amount of additive was added to the heated asphalt cement to produce the required asphalt cement-additive blend.
3. Three blends were prepared with 6, 10, and 15 percent Kraton by weight.
4. The blend was maintained hot to a goal temperature ranging between 160°C and 177°C (320°F and 350°F) for at least 2 hr.
5. The blend was thoroughly mixed by means of a low shear mechanical mixer for at least 15 min to obtain a more homogeneous blend.
6. Finally, the blend was kept at a temperature of 163°C (325°F) and ready for use.

#### Beam Preparation

The required percentages of aggregate were mixed in one batch to produce asphalt concrete beams with a target unit weight of 2386 kg/m<sup>3</sup> (149 pcf). The previously prepared Kraton-asphalt mixture was mixed with the same aggregate gradation to produce the three asphalt concrete cements tested. All beams contained 8 percent of asphalt cement as a percentage of the total mix. This percentage corresponds to the optimum asphalt cement content, as determined by the Marshall method of mix design (ASTM D1559-89). The aggregate mixes and the asphalt cement were heated to a temperature of about 177°C (350°F), along with the compaction mold and the mixing tools. The aggregate was then blended with the required amount of asphalt cement (8 percent of the total weight of mix) as quickly and thoroughly as possible to yield a mixture having a uniform distribution of asphalt cement. The heated mold was then filled with the heated asphalt cement-aggregate mixture. Static compaction was then performed by applying a uniform pressure of 13.79 MPa (2,000 psi) through a plate 0.051 × 0.38 m (2 × 15 in.) using a hydraulic press for 5 min. The overall dimension of each beam was 0.38 m long by 0.051 m wide by 0.089 m high (15 × 2 × 3.5 in.). The compacted beam was allowed to cool off in the mold for a few hours before it was removed and was usually tested 7 days after preparation and curing. Curing was achieved by maintaining the beams at 60°C (140°F) for 1 day.

### Laboratory Testing

#### Static Flexure Tests

Unnotched asphalt concrete beams were tested at room temperature [21°C (70°F)] under static flexure to determine the

ultimate flexural strength and the flexural modulus  $E$ . A screw-driven testing machine with a 22.24-kN (5,000-lb) load cell was used to conduct the static flexure tests on the beams subjected to symmetrical four-point loading. This load configuration produces an increasing static pure bending moment over the middle third of the beams 0.38 m (15 in.) long. The machine was provided with an upper fixed head and lower moving crosshead. The beam supporting fixture was attached to the crosshead with two end supports 0.26 m (10.2 in.) apart. The beam deflection was measured with a linear variable differential transducer, and the load deflection curve was recorded by means of an  $X$ - $Y$  plotter. After setting the beams on the supports and fitting the loading head on the top surface of the beam, the load was applied gradually at a constant rate of 4 mm/min (0.16 in./min) until failure was reached.

#### Fatigue Crack Propagation Tests

Four point bending fatigue crack propagation tests were performed under stress control using a repeated pneumatic flexure testing machine fitted with a 4.45-kN (1,000-lb) load cell. Tests were conducted in a laboratory environment at a constant temperature of about 21°C (70°F) using an invert haversine load. The load application period was 0.2 sec followed by a 2-sec rest period between repeated loads. As in the static flexural test, the support span was equal to 0.26 m (10.2 in.), and the distance between the midspan loading points was 0.086 m (3.4 in.). An initial straight notch 6.4 mm (0.25 in.) deep was inserted at the middle of the specimens with a 4-mm (0.156-in.) saw with a round tip of radius 2.4 mm (0.094 in.). A maximum load of 290 N (65 lb) was used with continuous cycle load applications from 0 to the maximum load. A hysteresis loop (load versus deflection) was recorded at 6.4-mm (0.25-in.) intervals of crack growth using the  $X$ - $Y$  plotter. Software was developed to digitize graphical data and to calculate pertinent areas within the load deflection curves obtained during fatigue testing.

## RESULTS AND DISCUSSION

### Static Flexural Behavior

Average values for three specimens tested at each set of conditions of the flexural modulus and ultimate bending strength for each mixture are shown in Table 1. Relationships

between the load and deflection for each mixture are shown in Figure 1. As the percentage of additive increases, both the ultimate flexural strength and the flexural modulus increase. This increase can be attributed to the strong elastic three-dimensional network formed by the polystyrene endblock domain of the modifier.

Thus, it appears that within the range of additive percentages tested, the hard polystyrene endblocks are enhancing the flexural ultimate strength and modulus. At the same time the rubbery midblocks are continuing to increase the toughness, as indicated by the increasing area under the load deflection curve in Figure 1. Increasing the percent of Kraton to more than 15 percent could stiffen the material, making it more brittle and less resistant to crack propagation with the polystyrene hard blocks dominating over the rubbery toughening midblocks. In practice, 6 percent or less additive by weight is commonly used. Although it is not economically feasible to add more than 6 percent additive, higher loadings of 10 and 15 percent were used to understand the fundamental changes in the mechanical behavior of modified asphalt concrete mixtures.

### Fatigue Crack Propagation Analysis

Relationships between the crack length ( $a$ ) and the number of cycles ( $N$ ) for each percentage of Kraton are shown in Figure 2. This figure indicates that for the 6 percent Kraton specimens, cracking began at about 1,800 cycles and advanced very rapidly, reaching its fatigue life at about 3,000 cycles. Cracking started at about 2,000 cycles in the 10 percent Kraton mixture and then advanced at a slower rate than in the 6 percent Kraton specimen, reaching its fatigue life at about 3,500 cycles. Finally, cracking started at about 2,000 cycles in the 15 percent Kraton mixture and advanced at a slower rate than in the 10 percent Kraton, reaching its fatigue life at about 3,800 cycles. The slope of the curves in Figure 2 is taken as the average crack speed at each crack length. Also, the propagation and initiation lifetimes are relatively greater in the case of the 15 percent Kraton than in the other two mixtures at the same stress level, whereas the 6 percent Kraton mixture has the shortest initiation and propagation lifetime.

Beams prepared from unmodified AC-5 asphalt cement and tested under the same set of conditions exhibited crack initiation at about 1,000 cycles. Lack of structural integrity and severe deformation on initiation did not allow for complete

TABLE 1 Mechanical Properties,  $\gamma'$ , and  $\beta'$  for Modified AC-5 with Various Kraton Contents

% Kraton in the AC-5 Mix	$E$ MPa (psi)	$\gamma'$ J/m <sup>3</sup> (in.-lb/in. <sup>3</sup> )	Bending Strength MPa (psi)	$\beta'$
6	49.6 (7200)	146.8±4.8 (2.13±0.07 × 10 <sup>-2</sup> )	1.04 (151)	2.61±0.09 × 10 <sup>-3</sup>
10	81.9 (11880)	188.2±11.7 (2.73±0.17 × 10 <sup>-2</sup> )	1.22 (177)	2.09±0.17 × 10 <sup>-3</sup>
15	142.5 (20661)	239.9±0.89 (3.48±0.013 × 10 <sup>-2</sup> )	1.88 (273)	1.44±0.05 × 10 <sup>-3</sup>

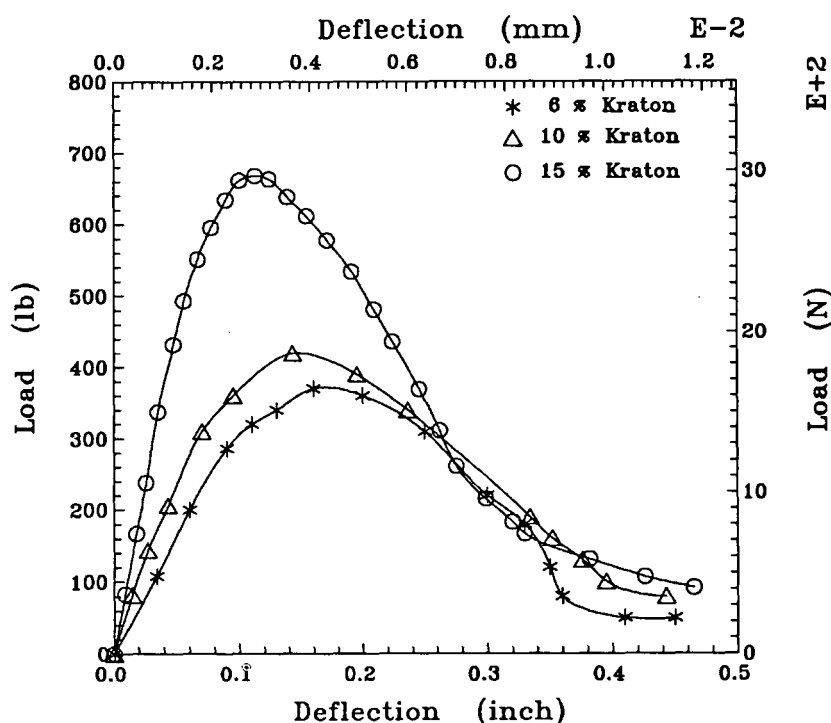


FIGURE 1 Load versus deflection of AC-5 mixture modified with various Kraton contents.

FCP tests. However, microstructural comparison between the unmodified and modified asphalt mixtures was made.

The energy release rate  $J^*$  was evaluated at increments of crack length from the area above the unloading curve (potential energy) of the hysteresis loops of each asphalt concrete mixture. Thus

$$J^* = \frac{\left(\frac{dP}{da}\right)}{B} \quad (2)$$

where

$P$  = potential energy,  
 $B$  = specimen thickness, and  
 $a$  = crack length.

The relationship between the average value (based on three identical specimens) of  $J^*$  and the crack length for each mixture is given in Figure 3. The average value of  $J^*$  for the 15 percent Kraton mixture is about 2 times higher than for the 6 percent Kraton mixture and 1.5 times higher than for the 10 percent Kraton mixture at the same crack length, which indicates the fracture resistance superiority of the 15 percent Kraton mixture. The value of  $J^*$  at each crack length is used in the present analysis to evaluate  $\gamma'$  and  $\beta'$  for each mixture.

The quantity  $\dot{W}_i$ , which is the "change in work," is measured directly as the area of the hysteresis loop at any crack length ( $a$ ) minus the area of the loop just before crack initiation. In viscoelastic materials,  $\dot{W}_i$  includes work expended on damage processes associated with crack growth and history-dependent viscous dissipation processes. Both processes are irreversible. The change in work  $\dot{W}_i$  versus the crack

length for typical beams tested from each mixture is shown in Figure 4. The value of  $\dot{W}_i$  for the 6 percent Kraton mixture is always higher than for the 10 and 15 percent Kraton mixtures. This is also demonstrated by the considerably larger size of the hysteresis loops recorded in the case of the 6 percent Kraton specimens compared with those of the 10 and 15 percent Kraton specimens. As shown in Figure 1, the addition of Kraton makes the binder less compliant because of the hard polystyrene endblocks, resulting in the decrease in the size of the hysteresis loops. Relationships between  $\dot{W}_i$  and the crack length ( $a$ ) are used in the evaluation of  $\gamma'$  and  $\beta'$ .

To evaluate the parameters  $\gamma'$  and  $\beta'$ , Equation 1 is rearranged as

$$\frac{J^*}{a} = \gamma' - \beta' \left[ \frac{\dot{W}_i}{\left(\frac{da}{dN}\right)a} \right] \quad (3)$$

A plot of the  $J^*/a$  versus  $[\dot{W}_i/(da/dN)a]$  for each of the three mixtures is shown in Figure 5, in which nearly all points plot along a straight line, from which  $\gamma'$  (the intercept) and  $\beta'$  (the slope) can be extracted. This is also observed in the other two identical specimens tested for each mixture. The average values of  $\gamma'$  and  $\beta'$  for each mixture are shown in Table 1. These results indicate that the average value of  $\gamma'$  for the 15 percent Kraton mixture is higher than that for the 10 and 6 percent Kraton mixtures. Thus, more energy is required to cause a unit volume of the 15 percent Kraton mixture to change from undamaged to damaged material, qualifying this mixture as the most resistant to crack propagation. In decreasing order, the 10 and the 6 percent Kraton mixtures follow. Also the lowest value of  $\beta'$  for the 15 percent Kraton

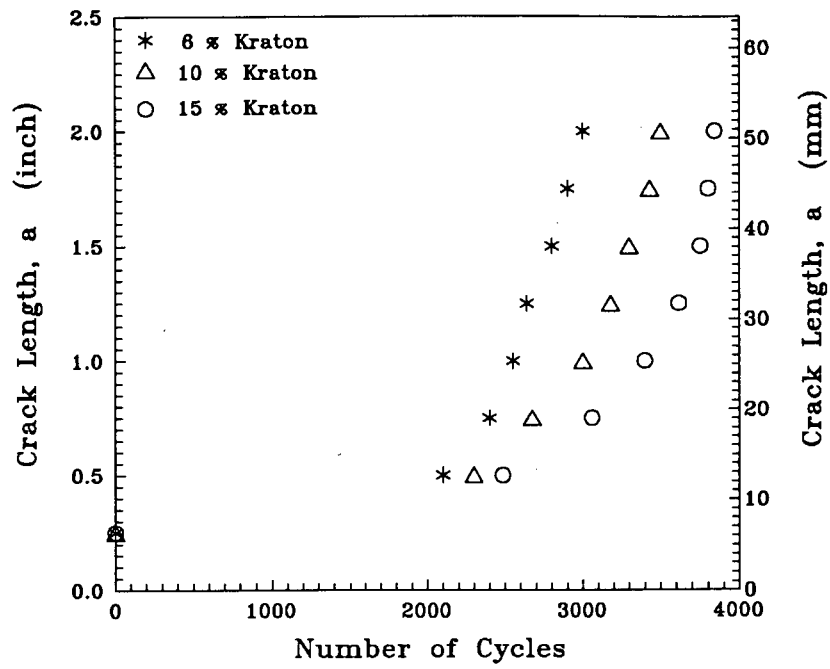


FIGURE 2 Crack length versus number of cycles.

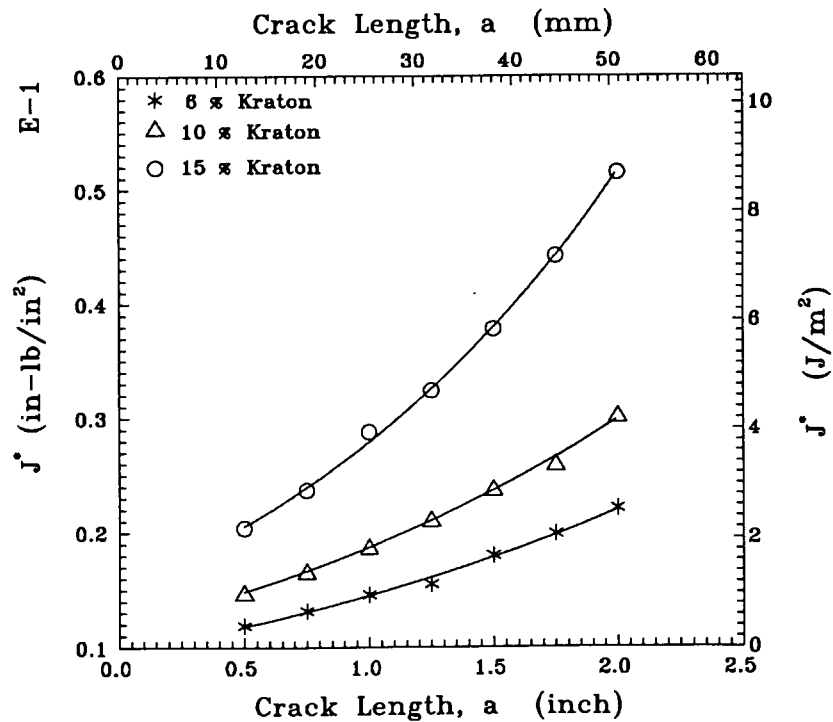


FIGURE 3 Energy release rate versus crack length for the AC-5 mixture modified with various Kraton contents.

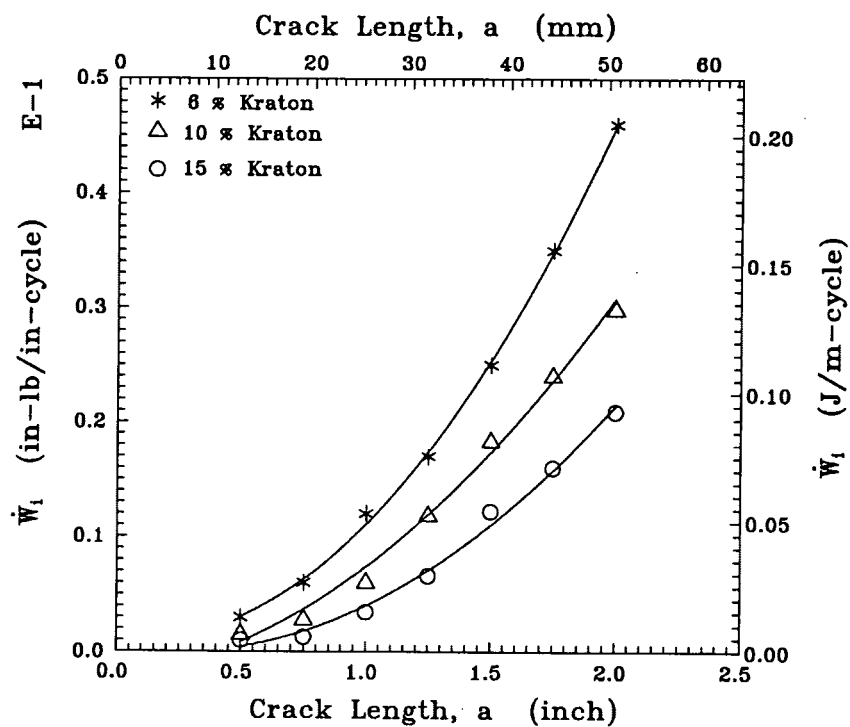


FIGURE 4 Change in work,  $\dot{W}_i$ , versus the crack length for static compacted AC-5 mixture modified with various Kraton contents.

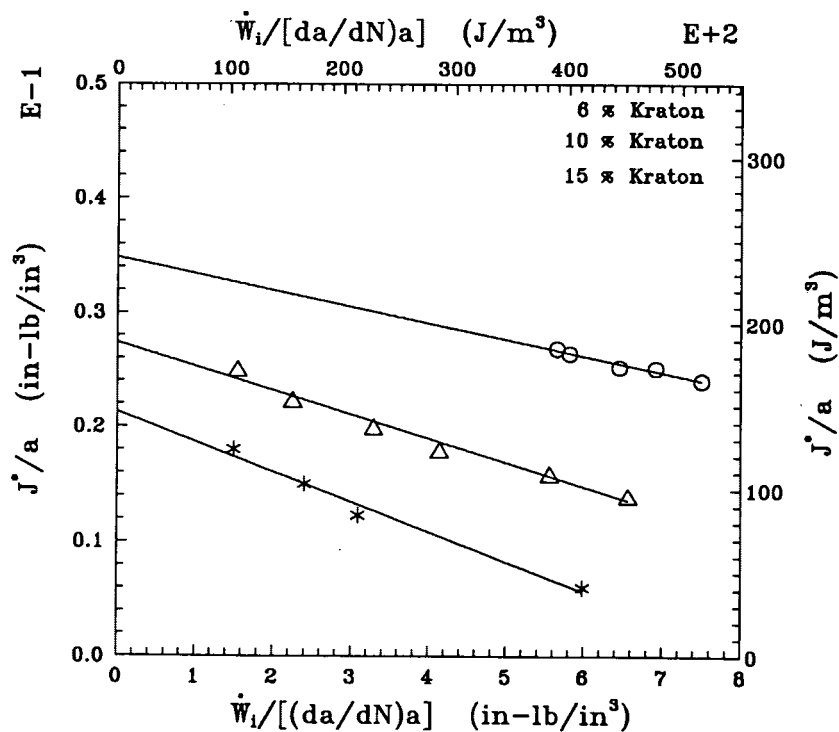


FIGURE 5 Fatigue crack propagation behavior of the AC-5 mixture modified with various Kraton contents plotted in the form of the MCL model to obtain  $\gamma'$  and  $\beta'$ .

mixture indicates that it possesses the least dissipative character followed by the 10 and the 6 percent asphalt concrete mixtures. Both a higher  $\gamma'$  and a lower  $\beta'$  in the case of the 15 percent Kraton mixture makes it more resistant to crack propagation, that is, tougher than the other two mixtures.

Similar studies on the effect of Elvax (ethylene vinyl acetate) modifier on the fatigue and fracture behavior of the AC-5 asphalt concrete mixture have been conducted by Othman (17). It was found that a 10 percent Elvax content had the maximum ultimate strength and maximum fracture toughness, on the basis of  $\gamma'$  and  $\beta'$ , compared with 6 and 15 percent Elvax content.

Plots of  $da/dN$  versus the energy release rate  $J^*$  for the three asphalt concrete mixtures under consideration (Figure 6) display the familiar S shape with three stages of crack propagation, particularly at 10 and 15 percent Kraton. The initial threshold stage is followed by a stage of reduced acceleration as the crack length increases, followed by a stage of critical crack propagation. The fatigue crack propagation curve is approximately linear in the second region, whereas in the third region the rate of fatigue crack propagation approaches its asymptotic value, where transition from stable to unstable conditions occurs.

The modified crack layer model is currently being used to study the effect of temperature, stress level, specimen geometry, and loading configurations on the resistance of asphalt concrete mixtures to fatigue crack propagation.

## SEM ANALYSIS

SEM analysis on the effect of Kraton modifier percentage reveals a distinct trend in the appearance of the fracture sur-

face, compared with that of the unmodified mixture (Figure 7) as the amount of modifier increases. These SEM samples are cut from the fracture surface of the specimen ahead of the initial notch. Because the Kraton modifier is being mixed initially with the hot asphalt, asphalt-rich areas from the fracture surface were examined.

At  $100\times$  magnification, a definite trend in the microstructural features (ridging) emerges. This ridging, which can be seen in Figures 8 through 10 for the 6, 10, and 15 percent mixtures, respectively, increases in both frequency and size as the percentage of Kraton in the asphalt increases. The increase in ridging formation in the asphalt-rich areas with the increase in additive percentage appears to be a result of the increased resistance of the matrix to surface separation. Better adhesion between the binder and the aggregate as well as better cohesion within the binder can result in microstretching of the binder, producing these ridges on the fracture surface.

Moreover, an increase in adhesion, induced by the increase in additive percentage in the AC-5 asphalt, is evident in Figures 11 through 13. In these micrographs at  $2,000\times$  magnification, the morphology of the fine aggregate particles is compared at different percentages of Kraton. These fine aggregate particles are well below the minimum sieve size used in this study. These are fine dust particles, which initially cling to the aggregate. They are then separated from the surface of the aggregate at the time of mixing with the hot liquid asphalt and become a particle phase in the pavement. At 0 percent Kraton, the surface of the particles appears to be very clean (Figure 11). At 10 percent Kraton (Figure 12) these particles appear to have a thicker coating than at 0 percent Kraton. At 15 percent Kraton (Figure 13) there is a dramatic

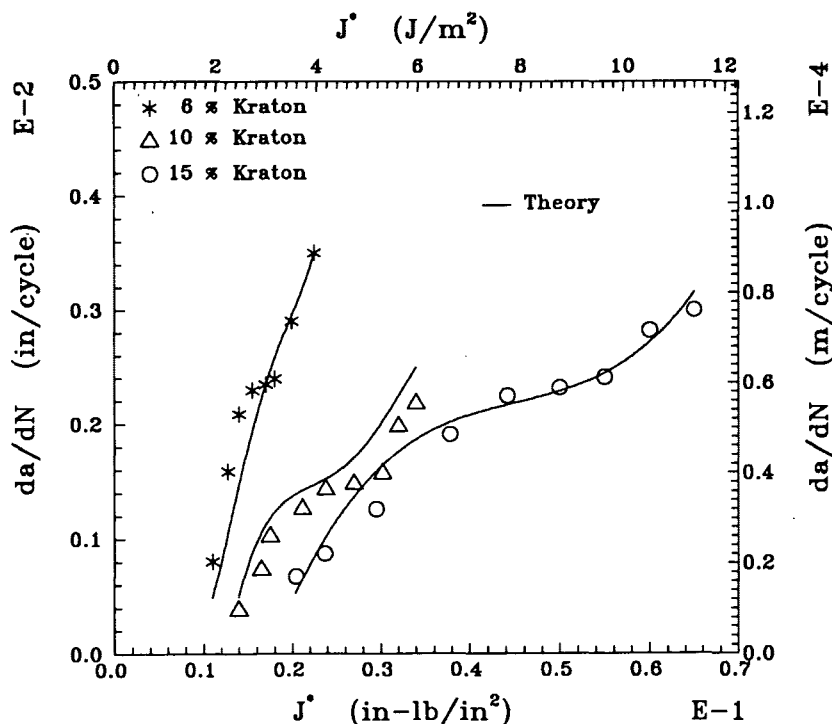
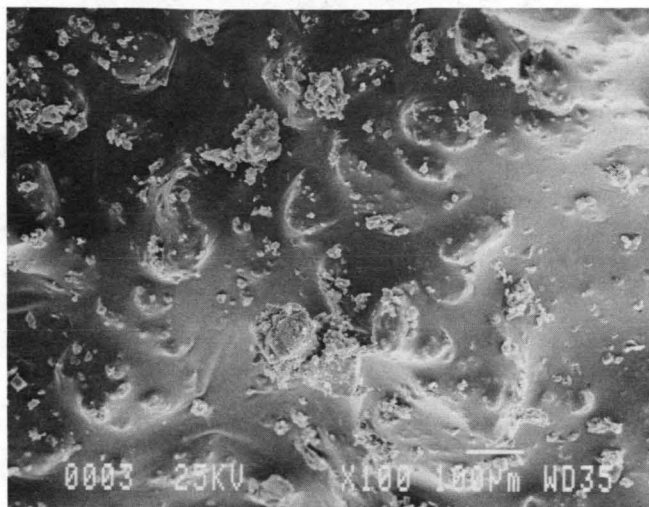
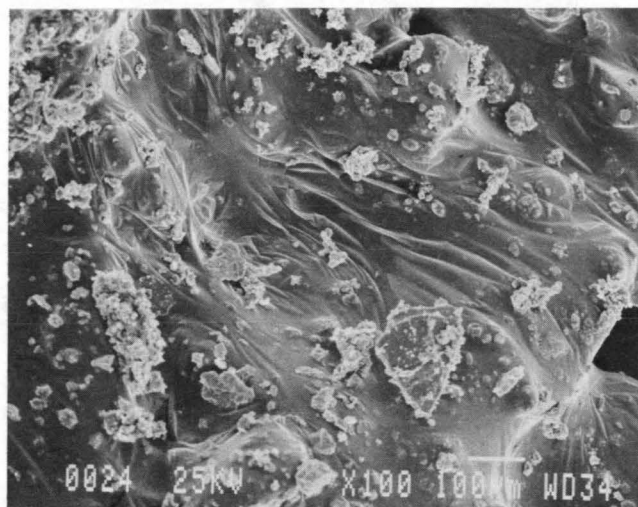


FIGURE 6 Theoretically predicted fatigue crack propagation speed based on the MCL model (with the experimental data) for the Kraton modified AC-5 mixtures with various Kraton contents.



**FIGURE 7** Microstructural features of an asphalt-rich area in the unmodified AC-5 mixture (0 percent Kraton).



**FIGURE 10** Microstructural features of an asphalt-rich area in the 15 percent Kraton modified AC-5 mixture.

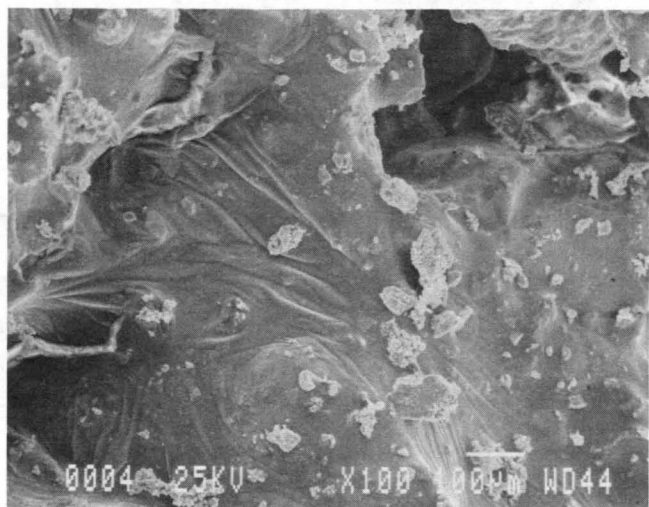


**FIGURE 8** Microstructural features of an asphalt-rich area in the 6 percent Kraton modified AC-5 mixture.

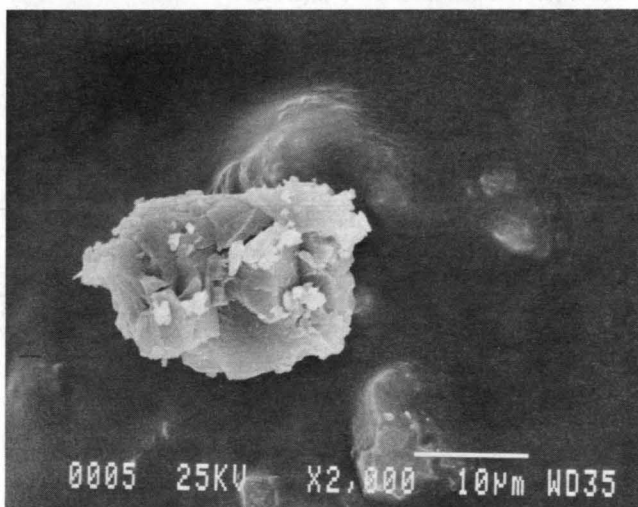


**FIGURE 11** Morphology of fine aggregate particles in the unmodified AC-5 mixture (0 percent Kraton).



**FIGURE 9** Microstructural features of an asphalt-rich area in the 10 percent Kraton modified AC-5 mixture.

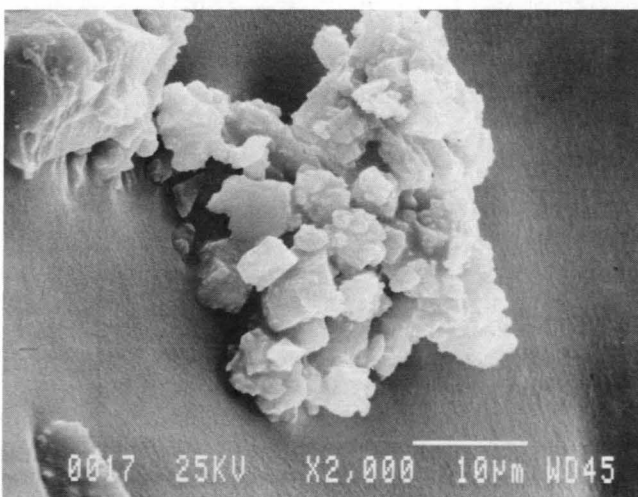


**FIGURE 12** Morphology of fine aggregate particles in the 10 percent Kraton modified AC-5 mixture.



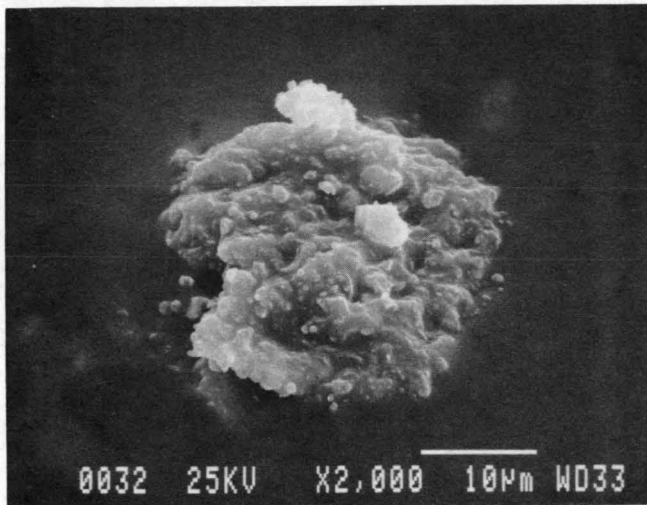


FIGURE 13 Morphology of fine aggregate particles in the 15 percent Kraton modified AC-5 mixture.

increase in the amount of binder adhered to the surface of these particles. This attests to the enhancement of the adhesive properties of the binder with the increase in the percentage of the Kraton modifier.

The interpretation of the SEM results appears to be in complete agreement with the results from both the flexural static and flexural fatigue investigations. As the percentage of the Kraton modifier increases, the ultimate strength and the flexural modulus increase. Also, the fracture toughness evaluated using the MCL model has increased, as indicated by higher  $\gamma'$  and lower  $\beta'$ .

### CONCLUDING REMARKS

Invoking the MCL model, the effect of SBS additive on the fatigue resistance of AC-5 asphalt concrete mixture has been studied. It was found that the specific energy of damage  $\gamma'$  increased with the increase in the Kraton percentage within the range tested (from 0 to 15 percent). The dissipation coefficient  $\beta'$  decreased with the increase in Kraton percentage. It was also found that both the ultimate flexural strength and modulus increased with the increase in Kraton percentage. The increase in the ultimate strength and fracture toughness is attributed to the contribution of the polystyrene hard endblocks and the soft butadiene rubbery midblocks, respectively.

The Kraton asphalt cement did not yield an optimum additive content up to 15 percent of the asphalt binder by weight. It may be that an increase in the SBS percentage will cause a decrease in the fracture toughness as the polystyrene hard endblocks become dominant, making the mixture more brittle. This point should be investigated further.

SEM analysis of the fracture surface revealed ridge formation in binder-rich areas that increased in size and intensity as the Kraton percentage increased. Better adhesion between

the binder and the aggregate as well as better cohesion within the binder results in microstretching of the binder, producing these ridges on the fracture surface. It is believed that this is the mechanism by which the Kraton-modified AC-5 asphalt concrete mixtures acquire their toughness.

### ACKNOWLEDGMENTS

This work was sponsored by the Army Corps of Engineers, Waterways Experiment Station, Vicksburg, Mississippi.

### REFERENCES

1. Key Facts About Polymer Modified Asphalt. *Better Roads*, July 1989.
2. Narusch, F. P. *Alaska Experience with Rubberized Asphalt Concrete Pavements, 1979–1982*. Division of Design and Construction, Alaska Department of Transportation and Public Facilities, Central Region, Aug. 1982.
3. Little, D. N. Performance Assessment of Binder-Rich Polyethylene Modified Asphalt Concrete Mixtures (Novophalt). Presented at 70th Annual Meeting of the Transportation Research Board, Washington, D.C., 1991.
4. Little, D. N., J. W. Button, et al. *Investigation of Asphalt Additives*. Report FHWA-R-D87/001. FHWA, U.S. Department of Transportation, 1986.
5. Wohler, A. *English Abstract in Engineering*, Vol. 2, 1871.
6. Paris, P., and F. Erdogan. A Critical Analysis of Crack Propagation Laws. *Journal of Basic Engineering*. In *Transactions ASME*, Vol. 85, 1963.
7. Paris, P. C., and C. G. Sih. Stress Analysis of Cracks. In *ASTM STP 381*, American Society for Testing and Materials, 1965, pp. 30–81.
8. Technical Product Specification, 6/89, sc:974-89, Shell Chemical Corp.
9. Technical Product Specification, 3m, 6/89, sc:937-89, Shell Chemical Corp.
10. Aglan, H. Evaluation of the Crack Layer Theory Employing a Linear Damage Evolution Approach. *International Journal of Damage Mech.*, Vol. 2, 1993.
11. Aglan, H., I. Shehata, L. Figueroa, and A. Othman. Structure-Fracture Toughness Relationships of Asphalt Concrete Mixtures. In *Transportation Research Record 1353*, TRB, National Research Council, Washington, D.C., 1992.
12. Aglan, H., and L. Figueroa. A Damage Evolution Approach to Fatigue Cracking in Pavements. *Journal of Engineering Mech.*, June 1993.
13. Aglan, H., M. Motuku, A. Othman, and L. Figueroa. Effect of Dynamic Compaction on the Fatigue Behavior of Asphalt Concrete Mixtures. Presented at 72nd Annual Meeting of the Transportation Research Board, Washington, D.C., 1993.
14. Chudnovsky, A. Crack Layer Theory. In *10th U.S. Conference on Applied Mech.* (J. P. Lamb, ed.), ASME, Houston, Tex., 1986.
15. Aglan, H., A. Chudnovsky, et al. Crack Layer Analysis of Fatigue Crack Propagation in Rubber Compounds. *Int. J. of Fract.*, Vol. 44, 1990.
16. *Construction and Materials Specifications*, Ohio Department of Transportation, Columbus, Jan. 1989.
17. Othman, A. *Fatigue Crack Propagation Behavior of Asphalt Concrete Mixtures*. M.S. thesis, Case Western Reserve University, Cleveland, Ohio, May 1992.

Publication of this paper sponsored by Committee on Characteristics of Bituminous Paving Mixtures To Meet Structural Requirements.